# Optical constants of evaporated amorphous zinc arsenide (Zn<sub>3</sub>As<sub>2</sub>) via spectroscopic ellipsometry

J. COLTER STEWART, MICAH N. SHELLEY, NATHAN R. SCHWARTZ, SPENCER K. KING, DANIEL W. BOYCE, JAMES W. ERIKSON, DAVID D. ALLRED,\* D AND JOHN S. COLTON

Department of Physics and Astronomy, Brigham Young University, Provo, UT 84602, USA \*dda@byu.edu

**Abstract:** We have used spectroscopic ellipsometry to measure the optical constants of evaporated amorphous zinc arsenide (Zn<sub>3</sub>As<sub>2</sub>). A five parameter model using a Tauc-Lorentz oscillator was found to fit well each of six amorphous samples deposited on Si<sub>3</sub>N<sub>4</sub>/silicon, allowing the layer thicknesses and optical constants to be deduced. Layer thicknesses varied from 20 to 70 nm. The fitted value of the optical gap (Tauc gap) is 0.95 eV, close to the 1.0 eV band gap for crystalline bulk zinc arsenide. A single set of parameters from an ensemble Tauc-Lorentz model can be used to determine the thicknesses of amorphous Zn<sub>3</sub>As<sub>2</sub> layers as long as the layers are  $\gtrsim$ 25 nm thick. Measured film thicknesses do not correlate with targeted thicknesses, likely due to low sticking coefficients of evaporated zinc arsenide.

© 2019 Optical Society of America under the terms of the OSA Open Access Publishing Agreement

#### 1. Introduction

Presently, gallium nitride (GaN) is used to produce many high-energy, high-temperature optical devices. However, zinc oxide (ZnO) has been recognized as a potentially cheaper alternative to GaN, possibly also with superior physical, electronic and optical properties [1]. A major obstacle in the optoelectronic commercialization of ZnO has proven to be naturally occurring defects such as lattice vacancies which cause nominally undoped material to be n-type, and compensate added p-type dopants. Reliable and reproducible heavily-doped p-type ZnO has not yet been commercialized [2]. Look et al. reported that good quality heavily p-type ZnO films could be produced by sputtering ZnO onto a hot zinc arsenide (Zn<sub>3</sub>As<sub>2</sub>)-coated substrate [3,4]. The Zn<sub>3</sub>As<sub>2</sub> coating was achieved by evaporation. Several p-type doped ZnO samples were produced which maintained their electrical properties after a decade. Our interest in thin-film zinc arsenide therefore arises out of its use as a source for arsenic doping of zinc oxide in this novel evaporation/sputter process.

Our research presented here has found that evaporated Zn<sub>3</sub>As<sub>2</sub> films are often amorphous, and in attempting to use spectroscopic ellipsometry to characterize the thickness of amorphous  $Zn_3As_2$  films, we have found the published optical constants of  $Zn_3As_2$  [5] to be inadequate. We have developed a Tauc-Lorentz oscillator model to fit our ellipsometric data which provides optical constants and allows thicknesses to be determined.

### Experimental technique

Zinc arsenide samples are made by evaporating powdered Zn<sub>3</sub>As<sub>2</sub> onto various substrates. Those samples are then characterized by scanning electron microscopy (SEM), X-ray diffraction (XRD), and variable-angle, spectroscopic ellipsometry (VASE).

### 2.1. Sample preparation

Powdered Zn<sub>3</sub>As<sub>2</sub> (Chemsavers ZNARSN100G, 99.9% grade) is placed in a tungsten boat (RD Mathis) in a Denton 502A Deposition System. The substrates are attached facing downward on a 10 cm diameter substrate holder using Kapton tape. This holder is located 23 cm above the boat and is attached to a chain-driven planetary system that rotates and rocks the holder in a quasi-nonrepeating pattern when energized. This evens out the deposited film thickness across the substrates. The chamber is closed and evacuated, typically to less than  $2 \times 10^{-6}$ torr and frequently to below  $5 \times 10^{-7}$  torr. Once the chamber has reached sufficiently low pressure, we begin to slowly ramp up the current, reaching approximately 120 amps in just over 1 min. At about 100 amps, a quartz crystal thin film deposition monitor (Inficon model XTM/2) indicates evaporation has commenced. This device monitors thickness by measuring the change in frequency of a quartz crystal resonator as a film is deposited. The substrate holder planetary, set at 0.33 revolutions/second, is activated, setting the substrate holder into motion. Once the target deposition rate of greater than 0.2 nm/s is reached, the shutter between the source and the substrate is opened and deposition on the substrate commences. Multiple substrates can be evaporated onto simultaneously. The deposition rate invariably increases substantially as the evaporation continues, and after reaching the pre-programmed thickness on the quartz crystal monitor, the shutter automatically closes. The chamber is then vented with dry nitrogen, and the coated substrates are removed and promptly taken to have their thicknesses measured via spectroscopic ellipsometry.

#### 2.2. Optical characterization

A J.A. Woollam M2000 variable-angle, spectroscopic ellipsometer is used to make measurements of thicknesses and optical constants. The usual substrates chosen for thickness determination are cleaved from 200 mm diameter, polished (100) Si test wafers coated with 300 nm (nominal thickness) CVD-grown silicon nitride (Si<sub>3</sub>N<sub>4</sub>) and are called "Si<sub>3</sub>N<sub>4</sub>/silicon" below. The rationale for using a layer of Si<sub>3</sub>N<sub>4</sub> for thickness and optical constants measurements comes from Hilfiker et al.'s work on characterizing thin absorbing films with spectroscopic ellipsometry [6]. They observed that it was difficult to measure the optical constants and thicknesses of thin absorbing materials deposited directly onto a silicon substrate. Ellipsometric measurements made on absorbing layers on silicon do not yield as reliable of thicknesses and optical constants as they do for transparent layers. Hilfiker et al. found that if a thin transparent spacer layer is added between an absorbing layer with unknown optical constants and the silicon substrate, then the ellipsometric measurements produce unique information as they would for a transparent film. Thus, we chose the following configuration for characterizing evaporated zinc arsenide (from top to bottom): an unknown thickness of Zn<sub>3</sub>As<sub>2</sub> (the partially absorbing layer), on 300 nm of Si<sub>3</sub>N<sub>4</sub> (the transparent spacer layer), on a silicon substrate. To say that the Zn<sub>3</sub>As<sub>2</sub> is partially absorbing means that over a portion of the energy range that the samples were studied, light could penetrate and reflect off the Zn<sub>3</sub>As<sub>2</sub>/Si<sub>3</sub>N<sub>4</sub> interface. This range is the portion below the material's optical gap, which at room temperature is about 1.0 eV for bulk Zn<sub>3</sub>As<sub>2</sub> [7]. In addition, as shown below, due to the thinness of the layers, the Zn<sub>3</sub>As<sub>2</sub> samples we prepared remain partially transparent for about 1.5 eV above this.

Ellipsometry measures the reflectivity of p- and s-polarized light. A measurement for a given wavelength and a given angle of incident light can be summarized by two parameters,  $\Psi$  and  $\Delta$ , for which the defining equation is:

$$\frac{r_p}{r_s} = \tan \Psi e^{i\Delta} \tag{1}$$

The parameters  $r_p$  and  $r_s$  are the reflection amplitude coefficients. Thus, the parameter  $\Psi$  describes the ratio of amplitudes of reflections from the two polarizations whereas the parameter  $\Delta$  describes the change in phase of the reflections. Measurements are done as a function of

wavelength at various incident angles. Specifically, in our case we have taken data with incident angles at  $5^{\circ}$  increments between  $60\text{-}80^{\circ}$  (all angles measured relative to the normal). That is, for every sample, for each of the five angles we obtain a set of measurements of the ellipsometric parameters,  $\Psi$  and  $\Delta$ , taken as functions of wavelength.

The angles that we measured were chosen to encompass the Brewster's angles of both silicon and silicon nitride, which in the visible range are about  $76^{\circ}$  and  $63^{\circ}$ , respectively [8]. Bulk  $Zn_3As_2$  is also expected to have its Brewster's angle in this range, at about  $77^{\circ}$  [5]. For a bulk material with little or no absorption,  $r_p$  vanishes at Brewster's angle so the ellipsometric parameter  $\Psi$  becomes zero or very small. This makes measurements close to Brewster's angle particularly useful in determining the optical constants of materials [9]. Assuming the optical constants of materials are known or can otherwise be determined, fits of the ellipsometric data can then be done to determine layer thicknesses.

In addition to the  $Si_3N_4$ /silicon substrates, we have also evaporated  $Zn_3As_2$  onto glass microscope slides and onto sapphire ( $Al_2O_3$ ) substrates. The sapphire substrates were chosen due to their potential of creating single crystal ZnO films as the ZnO lattice aligns itself with the oxygen sublattice in  $Al_2O_3$ , despite an 18% lattice mismatch [10]. Studying the  $Zn_3As_2$  films deposited on  $Si_3N_4$ /silicon and on glass was thus originally intended as a stepping stone to studying films on sapphire.

### 2.3. Structural measurements

In order to better understand the physical structure of our  $Zn_3As_2$  thin films, we measure surfaces with a Helios Nanolab 600 FEI scanning electron microscope (SEM) and perform X-ray diffraction (XRD) with a PANalytical X'Pert Pro MPD X-ray diffractometer at the Cu K $_{\alpha}$  line. The XRD yields information about differences in crystallinity between samples, and the SEM gives structural information and provides a check on the roughness information obtained from ellipsometry.

#### 3. Results and discussion

#### 3.1. Structural

 $Zn_3As_2$  films on sapphire and on  $Si_3N_4/silicon$  were examined by SEM. Figures 1(a) and (b) show representative micrographs of films grown on these two types of substrates, respectively. The magnification of each picture was adjusted so that the picture is 1  $\mu$ m<sup>2</sup> area of the samples.

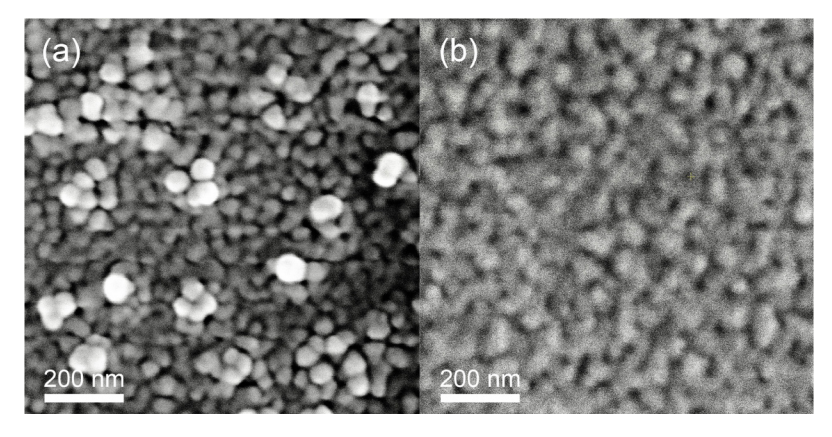


**Fig. 1.** Representative SEM images of  $Zn_3As_2$  samples on (a) sapphire and (b)  $Si_3N_4$ /silicon (right). Each image displays a 1  $\mu$ m<sup>2</sup> area of the samples.

Figure 1(a) shows the formation of polycrystalline  $Zn_3As_2$  on a sapphire substrate, likely via an island-growth mechanism such as Volmer–Weber (VW) growth although the Stranski–Krastanov mechanism cannot be ruled out [11,12]. VW growth occurs when atoms or molecules in the evaporant are more strongly bound to each other than to substrate atoms, and is often seen in the growth of semiconductors on oxides [11] as is the case here.

As seen in Fig. 1(a), the  $Zn_3As_2$  deposited on sapphire is composed mainly of many small, distinct masses, roughly 30-50 nm in size. Most are separated from some of their neighbors by voids or high-aspect-ratio cracks. This surface is noticeably rougher than the  $Zn_3As_2$  grown on  $Si_3N_4$ /silicon, shown in Fig. 1(b). In addition, there are numerous grains whose top surfaces appear to lie above most others. These are larger and appear bright in the micrograph. This may be evidence of competitive growth with certain preferred crystallographic growth planes, which is common in thin-film growth. Several of the larger, isolated grains possess a hexagonal habit. In several spots, approximately equal-sized grains come together with angles of approximately  $120^{\circ}$  and are positioned relative to one another suggesting underlying symmetry templating their growth. This is suggestive of the (111) planes of a cubic crystal. Many smaller grains come together with  $90^{\circ}$  angles, while acute angles including  $60^{\circ}$  can also be seen. Previous investigators have noted that  $Zn_3As_2$  had a rough surface when grown on a crystalline substrate; in their case this was done by metalorganic vapor-phase epitaxy (MOVPE) on InP [13].

On the other hand, the sample on  $Si_3N_4$  shown in Fig. 1(b) is observed to have an "orange-peel" surface texture with curved surfaces, one feature flowing into another. (This was sample D, see Table 1 below.) Little evidence of crystallinity is seen. In fact, XRD spectra of samples on  $Si_3N_4$ /silicon and on glass substrates show they are amorphous; there are no peaks aside from those due to the (100) silicon substrate. That the films on  $Si_3N_4$ /silicon and on glass are amorphous is not too surprising; both glass and the  $Si_3N_4$  layer on silicon are themselves amorphous. Moreover, arsenic is a glass-forming element in chalcogenide glasses. For example, arsenic trisulfide ( $As_2S_3$ ) is usually amorphous as prepared [14]. By contrast, XRD spectra from samples on sapphire show multiple large peaks in addition to those due to the sapphire substrate, evidence that the material is polycrystalline. There is also evidence of preferred orientation of the  $Zn_3As_2$  layers on sapphire, which is discussed more fully elsewhere [15].

Table 1. Thicknesses (nm) and Roughnesses (nm) of  $\text{Zn}_3\text{As}_2$  layers on  $\text{Si}_3\text{N}_4/\text{silicon}$ .

Sample	Thickness Monitor Programmed Thickness	Individual Model Fits			Ensemble Model Fit		
		Ellipsometry Thickness	Roughness	MSE	Ellipsometry Thickness	Roughness	MSE
A	200	21.6	7.6	8.8	16.2	9.0	63.9
В	230	51.6	7.2	7.8	52.0	7.2	35.5
C	100	30.6	8.9	9.6	28.5	11.4	61.5
D	250	36.2	12.3	8.3	33.8	12.8	27.5
E	244	71.3	11.8	7.1	72.7	12.4	51.4
F	50	23.8	10.1	16.3	19.8	11.5	53.8
Average Standard Deviation			9.7	9.6		10.7	48.9
			2.0	3.1		2.0	3.1

### 3.2. Spectroscopic ellipsometry

In Fig. 2 we show representative ellipsometric data:  $\Psi$  and  $\Delta$  measured at 70° for a sample grown on Si<sub>3</sub>N<sub>4</sub>/silicon. (This was sample E, see Table 1 below.) The solid blue line is the measured data for  $\Psi$  and the solid red line is the measured data for  $\Delta$ . Model-generated data as explained

below is overlaid on each plot with dashed lines. The example shown was deliberately chosen to not be an optimum fit, in order to more clearly show the differences between experimental and model-generated values. The curves in Fig. 2 are marked by oscillations at energies below about 2.5 eV (above 450 nm), while above 2.5 eV (below 450 nm)  $\Psi$  gradually increases. The position of the oscillations is determined primarily by the thickness of the 300 nm Si<sub>3</sub>N<sub>4</sub> layer, while their amplitude and width are determined primarily by the absorption of the zinc arsenide layer. The ellipsometric spectrum of an uncoated silicon nitride sample shows narrower peaks with higher contrast [16].

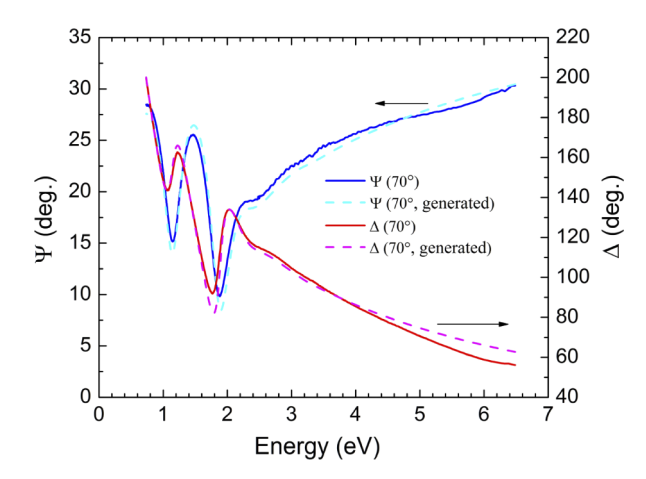


**Fig. 2.** Representative  $\Psi$  and  $\Delta$  values as a function of photon energy, measured at 70° for a sample of Zn<sub>3</sub>As<sub>2</sub> on Si<sub>3</sub>N<sub>4</sub>/silicon. The solid lines represent experimental data. The model-generated data (deliberately chosen to be a non-optimum fit) is overlaid on each plot with dashed lines.

Optical constants for bulk, crystalline  $Zn_3As_2$  are available from Handbook of Optical Constants of Solids, III, and references cited therein [5]. These literature values were obtained by bulk reflectivity measurements, after which Kramers-Kronig (K-K) analysis was employed to obtain the optical constants. We first attempted to fit our ellipsometric data using these optical constants from the literature; however, this was unsuccessful. Therefore, as is standard for VASE, we modeled the optical constants of our films using a suite of oscillators. We selected various oscillators from J.A. Woollam's variable-angle spectroscopic ellipsometry software (WVASE) to build trial models. The aim with these trial models is to find a common set of parameters, called an ensemble model, that can be used to specify the optical constants of all of the evaporated films to facilitate thickness measurements. This is done by first fitting a model for each sample individually, and then allowing the model to adjust its parameters while fitting multiple samples simultaneously.

We found that the ellipsometric data of  $Zn_3As_2$  on  $Si_3N_4$ /silicon for any individual sample could be well modeled, for the purpose of measuring thicknesses, with Woollam's general oscillator approach. The model consisted of three layers on a silicon substrate, namely (from bottom to top) a silicon substrate, a  $Si_3N_4$  layer, a  $Zn_3As_2$  layer, and finally a layer of  $Zn_3As_2$  roughness. Roughness is defined as 50% underlayer material mixed with 50% void. The optical constants of the  $Si_3N_4$  had previously been determined and were not allowed to vary. However, the  $Si_3N_4$  thickness for a given sample was not precisely known and therefore was allowed to vary from 302 to 310 nm. For the  $Zn_3As_2$  layers we found that a five parameter model could fit the data for each sample individually: a four parameter Tauc-Lorentz (TL) oscillator along with the value of  $\varepsilon_1$  (the real part of the complex relative permittivity) at  $E = \infty$ .

The Tauc-Lorentz oscillator model is particularly well suited for amorphous materials. Tauc et al. proposed a model for understanding the optical gap of disordered materials by considering the general form of the joint density of states (JDOS) near the optical gap of disordered materials [17,18]. The optical gap for amorphous materials, also called the Tauc gap, is similar to crystalline materials' band gap. This description is adequate to describe the interaction of light near the band edges but is not K-K consistent. Jellison et al. derived a parametric model of the dielectric function of semiconductor and dielectric materials which added Lorentz (classical) oscillator broadening to Tauc's optical-gap approach, to obtain an optical JDOS [19]. With additional approximations concerning momentum transfer, etc., the TL model is generated [19,20].

The Tauc-Lorentz oscillator model calculates the relative permittivity function  $\varepsilon = \varepsilon_1 + i\varepsilon_2$  of a material, where:

$$\varepsilon_{2} = \begin{cases} \frac{A E_{0} C(E - E_{g})^{2}}{(E^{2} - E_{0}^{2})^{2} + C^{2}E^{2}} \cdot \frac{1}{E}, & E > E_{g} \\ 0, & E \leq E_{g} \end{cases}$$

$$\varepsilon_{1} = \frac{2}{\pi} P \int_{E_{g}}^{\infty} \frac{\xi \varepsilon_{2}(\xi)}{\xi^{2} - E^{2}} d\xi + \varepsilon_{1}(\infty)$$
(2)

Here,  $\varepsilon_2$  represents an absorption peak described by four parameters: A represents the amplitude of the peak,  $E_0$  is a measure of the central energy of the peak,  $E_g$  is the optical gap, and C is a measure of the peak width. The equation for  $\varepsilon_1$  comes from the K-K transform of  $\varepsilon_2$ , with the fifth fitting parameter  $\varepsilon_1(\infty)$  explicitly added in. The real and imaginary optical constants n and k can be calculated in the usual way from  $\varepsilon_1$  and  $\varepsilon_2$  (and vice versa) using the formulas

$$n + ik = \sqrt{\varepsilon_1 + i\varepsilon_2}$$

$$\varepsilon_1 = n^2 - k^2, \text{ and}$$

$$\varepsilon_2 = 2nk.$$
(3)

Since there are approximately 700 values of  $\Psi$  and  $\Delta$  per measurement angle, this is a vastly overdetermined system.

The Cody-Lorentz (CL) oscillator model was also examined. This oscillator, like the Tauc-Lorentz oscillator, is designed specifically for amorphous semiconductors [20–22]. Though the model incorporates more adjustable parameters than the TL model, the fits obtained were not significantly different than those from the TL model, nor was the mean-squared error (MSE) of the CL fits any better. Thus, we judged the Tauc-Lorentz oscillator to be sufficient for our purposes.

For each sample, the thickness and roughness of the zinc arsenide, the five TL model parameters, and the  $Si_3N_4$  thickness were allowed to vary. The results of the fits not only yield the  $Zn_3As_2$  layer thicknesses and roughnesses, but also (through Eqs. (2) and (3)) the optical constants of zinc arsenide. Sample-specific fits generally result in an MSE of less than 10. The MSE is an average of the squared difference between the model-generated data and the experimental data, weighted by the inverse error bar squared for each data point (so noisy points are weighted less heavily).

Table 1 shows the fitted thickness and roughness values for six samples of  $Zn_3As_2$  on  $Si_3N_4$ /silicon, labeled samples A-F. The "Thickness Monitor Programmed Thickness" column indicates the targeted thickness via the Inficon quartz crystal monitor whereas the "Ellipsometry thickness" column is the value from the TL fits. The right three columns contain values obtained by fitting each sample to the ensemble model, discussed in more detail below.

The samples are all quite rough. The average roughness given by ellipsometry is fairly consistently about 10 nm, independent of thickness. Thus for the thinnest samples, the roughness comprises a significant fraction of the overall layer thickness. These values of the roughness are not inconsistent with SEM results.

#### 3.3. Growth nucleation

There is perhaps surprisingly no correlation in Table 1 between a given sample's thickness according to the quartz crystal monitor and its thickness determined by ellipsometry. In no case was the film as thick as the monitor indicated. In addition, the ratio between the two thicknesses varied considerably. Even with the same target thickness set on the quartz crystal monitor, two independent evaporations could come out with vastly different thicknesses of  $Zn_3As_2$ . Moreover, some of our samples (not shown in the table) emerged with no detectible  $Zn_3As_2$  on them at all.

This lack of correlation between targeted and measured thicknesses is likely related to sticking (or condensation) coefficients and other details relating to nucleation and growth. A sticking coefficient for atoms incident on a surface is the ratio of atoms which stick to the surface to the total number of incident atoms. As explained in the capillary model of thin film nucleation, in the initial stages of deposition many atoms which strike a surface before nucleation has occurred will reevaporate from the surface [11]. Within this model,  $Zn_3As_2$  films will only appear on the substrates after stable nucleation sites have appeared. If a collection of zinc arsenide molecules stick together on the substrate, a film forms that grows outward and thicker, but if an atom or molecule never finds a site to stick to other atoms, then the atoms eventually reevaporate and the sample comes out clean of any films.

The sticking coefficient for atoms on substrates can vary from close to zero (for substrates at very high temperatures) to close to one (for substrates at lower temperatures) [23]. For a given atom, the temperature dependence can also vary substantially on the type of substrate, as for example has been reported for silver atoms on ruthenium, oxygen-modified ruthenium surfaces, sapphire, and alumina film (random orientation) [24].

The sticking coefficient for zinc atoms on silver has been reported to be close to unity at 341 K [25]. The sticking coefficient of group V elements (e.g. As, etc.) has been a subject of great interest because of its importance in the deposition of III-V compounds by molecular beam epitaxy (MBE). Within that context, previous research has determined desorption constants and sticking coefficients of As on GaAs surfaces as a function of temperature via experimental data combined with an atomistic model (sticking coefficients between 0.1 and 0.9). However, these previous studies are not directly applicable for our case, because we evaporate the Zn and As atoms together, and sticking coefficients for zinc arsenide have not been reported for any substrates.

To investigate this as a possible phenomenon, we placed a small video camera and light source in the evaporation chamber to record the growth of layers on the substrates. (For these videos, substrate rotation via planetary was not used.) We discovered that after the shutter is opened, many seconds elapse before the substrate shows the presence of any Zn<sub>3</sub>As<sub>2</sub> layer growth; the presence of a Zn<sub>3</sub>As<sub>2</sub> layer could be judged by a darkening of the substrate. As indicated by this darkening, the zinc arsenide film appears first at a single spot on the surface and then spreads outwards. The amount of time prior to darkening is highly variable, and significantly, the darkening of two different substrates placed side-by-side begins at different times and proceeds at different rates. Figure 3 shows a still frame from one of these evaporation videos; in it we see that the substrate on the left, a glass slide, has begun to darken before the right-hand sapphire substrate. This provides evidence that surface nucleation during evaporation occurs at random times after the shutter is opened, and explains the differences between targeted and measured film thicknesses. This can be understood in a model where the sticking coefficient of zinc arsenide on itself is close to one, while the sticking coefficient of zinc arsenic on these substrates is very small. Specific nucleation sites could also often be identified in these videos by the outward spread of the darkening; what is unusual here is that the nucleation—an atomic scale event—occurs only in one small area over a macroscopically large (many cm<sup>2</sup>) area surface.

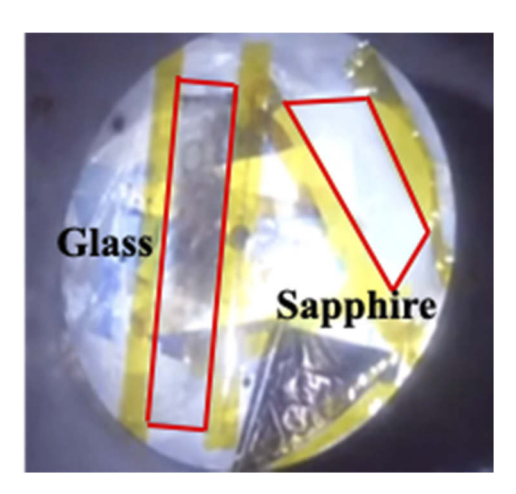


**Fig. 3.** Still photo extracted from growth video during evaporation. The dark gray indicating  $Zn_3As_2$  film growth develops on the left-hand substrate (glass) before it does on the right-hand substrate (sapphire). See **Visualization 1** for a video of the growth (3× speed) which begins 3:20 after nominal start of evaporation. The amount of time from start of evaporation to darkening is highly variable from sample to sample.

#### 3.4. Ensemble ellipsometric fits

Each sample listed in Table 1 required slightly different parameters for best fitting with the TL model. It is well known that the optical properties of many amorphous semiconductors vary from sample to sample, which is evidence that, in contrast with crystalline materials, there is not a single best "amorphous state" [26]. Thus, it is not particularly surprising that the fit parameters, and hence the optical constants, of the amorphous  $Zn_3As_2$  layers on  $Si_3N_4$ /silicon vary from sample to sample. However, it is possible that these variations could result from a dependence of the optical constants on layer thickness. Therefore, it was desirable to see if parameters for an "average" TL model could be extracted that could adequately model the ellipsometric data from all samples A-F, regardless of thickness.

To accomplish this, we fitted the ellipsometric data from all six samples together in an ensemble model where the TL model's five parameters were not allowed to vary from sample to sample. (By contrast, the  $Zn_3As_2$  thicknesses and roughnesses as well as the  $Si_3N_4$  thicknesses were still allowed to be sample dependent.) This approach is termed multisample analysis, and can reduce parameter-parameter and parameter-thickness correlation effects, as well as increase parameter accuracy if the optical constants of the thin films are not thickness dependent [27]. We display the value of the parameters generated by this approach in Table 2.

Table 2. TL model parameter values from an ensemble fit of the six amorphous  $Zn_3As_2$  on  $Si_3N_4/silicon$  samples.

Parameter	Value
$\overline{A}$	$129.0 \pm 0.6 \text{ eV}$
$E_0$	$3.167 \pm 0.004 \text{ eV}$
$E_g$	$0.952 \pm 0.002 \text{ eV}$
C	$4.01 \pm 0.01 \text{ eV}$
$arepsilon_1(\infty)$	$1.52 \pm 0.02$

The layer thicknesses, roughnesses, and MSEs for samples A-F from the ensemble fit are displayed in Table 1 and can be compared to those values from the individual fits. The ensemble

model caused the MSE to increase from an average of 9.6 to an average of 48.9. This increase in MSE is sufficiently large to negate the hypothesis that the material in all six samples is the same. However, as to the question of whether the optical constants obtained by the ensemble approach can be used to find the thicknesses of the films, the answer is generally yes. For the thickest films, there is a very good agreement between the thicknesses obtained through individual fits vs. the ensemble fit. The roughnesses also have generally good agreement. For the purpose of comparing the two types of fits, we compute an effective thickness as the sum of the thickness plus half of the roughness. The difference in effective thicknesses for samples B, C, D, and E is 5% or less. For samples A and F (the thinnest samples) it is 19% and 11%, respectively. Thus, we conclude that unless the layers are particularly thin ( $\lesssim 25 \text{ nm}$ ), the amorphous Zn<sub>3</sub>As<sub>2</sub> layer thicknesses can be well estimated by using the ensemble TL model fit parameters given in Table 2.

The fit parameters from Table 2 can therefore be used in Eqs. (2) and (3) to compute the optical constants of an "average" amorphous  $Zn_3As_2$  layer. These optical constants, n and k, are plotted in Fig. 4, along with literature values for crystalline bulk  $Zn_3As_2$  from Ref. [5]. The smoothness of our curve compared to the literature curve is to be expected since our optical constants come from an oscillator model which is only capable of generating smooth functions. Note, however, that our smooth functions do a much better job in the ellipsometry fits of the amorphous samples than do the literature values, and they depart from the literature values in significant ways (as can be seen in the figure). To give an idea of the uncertainty of the ensemble fit, we have also analyzed the n and k values obtained from the individual model fits referred to in Table 1; the shaded portions of the graph indicate confidence intervals created from average values from those fits, plus/minus one standard deviation.

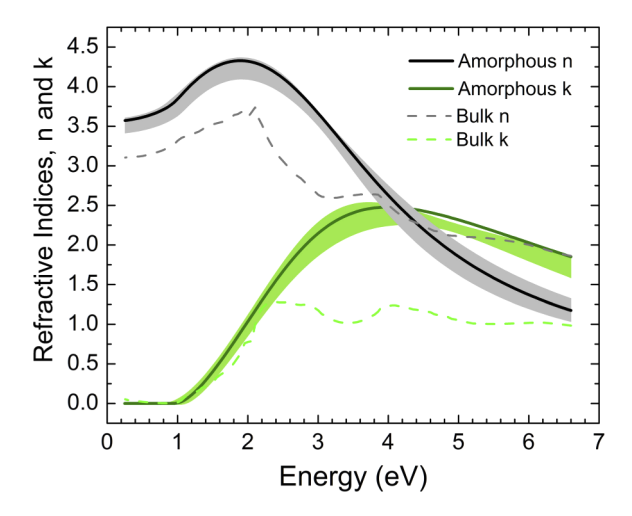


**Fig. 4.** Optical constants (n and k) for our ensemble fit of six amorphous samples of  $Zn_3As_2$  on  $Si_3N_4$ /silicon, compared to values for crystalline bulk  $Zn_3As_2$  from Ref. [5]. Note that the ellipsometry data for the amorphous material was only taken at energies from 0.7 to 6.5 eV; n and k values for energies outside that range should be considered an extrapolation. The shaded portions of the graph indicate confidence intervals created from average values of n and k from the individual model fits, plus/minus one standard deviation. See Data File 1 for underlying values for the amorphous material.

 $E_g$  in Table 2 is the optical gap for our average amorphous  $Zn_3As_2$  layer as determined by our ensemble fit. We note that it is close to the value of 1.0 eV for the room temperature band gap of crystalline  $Zn_2As_3$  [7]. As an alternate method of calculating  $E_g$  for the amorphous  $Zn_3As_2$  material, we have also done an ensemble fit of the ellipsometry data starting with the n and k

values from the TL model but then allowing n and k to vary from there. We then did a Tauc plot of  $\varepsilon_2$  (= 2nk), which is proportional to the absorption; when plotted as  $(\varepsilon_2 E_{photon})^{1/2}$  it displays a linear onset of absorption whose x-axis intercept is the band gap.  $E_g$  obtained via that method is 0.98 eV, in close agreement to the  $E_g$  fitting parameter of the TL oscillator model, 0.95 eV.

To test whether our ensemble model works well for amorphous  $Zn_3As_2$  layers in general, we tested it with several samples of amorphous  $Zn_3As_2$  grown on glass. Using the ensemble model n and k values and leaving only the  $Zn_3As_2$  layer thickness and roughness as adjustable parameters, we were able to fit ellipsometric data for amorphous  $Zn_3As_2$  layers on glass with MSE values similar to the ensemble model MSE values found in Table 1. Allowing the TL model parameters to vary for individual sample fits yielded MSE values similar to the individual fit MSE values in Table 1. By contrast, attempts to use our ensemble model with  $Zn_3As_2$  layers on sapphire failed; the MSE increased substantially. As discussed above, these are polycrystalline samples and are therefore expected to have different optical constants; the morphology of these samples also give rise to roughnesses comparable to the thicknesses of the films, which adds to the difficulty.

### 4. Summary and conclusions

Evaporated  $Zn_3As_2$  layers deposited on  $Si_3N_4$ /silicon and on glass were determined to be amorphous by XRD and SEM, whereas  $Zn_3As_2$  layers on sapphire are polycrystalline. Film thicknesses do not correlate with quartz crystal monitor values, likely due to nucleation of film growth occurring at random times after evaporation has begun as a result of the low sticking coefficient of evaporated zinc arsenide to the substrates.

Six samples grown on  $Si_3N_4$ /silicon were examined in detail by ellipsometry. Their roughness is about 10 nm, independent of thickness. The optical constants for all of these are well described by a Tauc-Lorentz model of the  $Zn_3As_2$ , with slightly varying parameters for their individual fits. A single set of parameters from the TL model and the optical constants derived from those parameters can be used to describe an "average" amorphous sample, and to determine the thicknesses of amorphous  $Zn_3As_2$  layers as long as the layers are  $\gtrsim 25$  nm thick. The optical gap given by the ensemble model is 0.95 eV, close to the 1.0 eV value for bulk zinc arsenide. The parameters/optical constants from the ensemble model also act as a good starting point for fitting samples using individual TL models. The TL model, however, does not work well for  $Zn_3As_2$  grown on sapphire, likely due to the polycrystalline and rough nature of those films.

### **Acknowledgments**

We thank John E. Ellsworth for assistance with the Denton vacuum system, Jeff Farrer for assistance with the SEM imaging, Stacy Smith for assistance in making XRD measurements and Prof. Matthew Linford and his students for assistance and guidance in using the M2000 spectroscopic ellipsometer.

#### **Disclosures**

The authors declare no conflicts of interest.

#### References

- Ü Ozgur, D. Hofstetter, and H. Morkoç, "ZnO devices and applications: A review of current status and future prospects," Proc. IEEE 98(7), 1255–1268 (2010).
- D. C. Look, B. Claffin, Y. I. Alivov, and S. J. Park, "The future of ZnO light emitters," Phys. Status Solidi C 201(10), 2203–2212 (2004).
- 3. D. C. Look, G. M. Renlund, R. H. Burgener, and J. R. Sizelove, "As-doped p-type ZnO produced by an evaporation/sputtering process," Appl. Phys. Lett. 85(22), 5269–5271 (2004).
- 4. R. H. Burgener, R. L. Felix, and G. M. Renlund, "Fabrication of P-type Group II-VI Semiconductors," U.S. patent US 7141489 B2 (2006).

- J. Misiewicz and K. Jezierski, "Zinc Arsenide (Zn3As2)," in Handbook of Optical Constants of Solids, III, E. D. Palik, ed. (Academic Press, 1998), pp. 595–607.
- J. N. Hilfiker, N. Singh, T. Tiwald, D. Convey, S. M. Smith, J. H. Baker, and H. G. Tompkins, "Survey of methods to characterize thin absorbing films with Spectroscopic Ellipsometry," Thin Solid Films 516(22), 7979–7989 (2008).
- 7. J. Misiewicz and J. M. Pawlikowski, "Optical band-gap of Zn3As2," Solid State Commun. 32(8), 687-690 (1979).
- 8. D. E. Aspnes and A. A. Studna, "Dielectric functions and optical parameters of Si, Ge, GaP, GaAs, GaSb, InP, InAs, and InSb from 1.5 to 6.0 eV," Phys. Rev. B 27(2), 985–1009 (1983).
- 9. M. Schubert, "Theory and Application of Generalized Ellipsometry," in *Handbook of Ellipsometry*, H. G. Tompkins and E. A. Irene, eds. (Springer, 2005), pp. 691–692.
- Y. Chen, D. M. Bagnall, H. J. Koh, K. T. Park, K. Hiraga, Z. Zhu, and T. Yao, "Plasma assisted molecular beam epitaxy of ZnO on c-plane sapphire: Growth and characterization," J. Appl. Phys. 84(7), 3912–3918 (1998).
- 11. M. Ohring, "Substrate Surfaces and Thin-Film Nucleation," in *Materials Science of Thin Films: Deposition and Structure*, 2nd ed. (Academic Press, 2002), pp. 357–415.
- I. N. Stranski and L. Krastanow, "Zur Theorie der orientierten Ausscheidung von Ionenkristallen aufeinander," Monatsh. Chem. 71(1), 351–364 (1937).
- D. J. Brink and J. A. A. Engelbrecht, "Ellipsometric investigation of rough zinc arsenide epilayers," Appl. Opt. 41(10), 1894 (2002).
- F. W. Glaze, D. H. Blackburn, J. S. Osmalov, D. Hubbard, and M. H. Black, "Properties of arsenic sulfide glass," J. Res. Natl. Bur. Stand. 59(2), 83 (1957).
- 15. M. N. Shelley, S. K. King, B. J. Campbell, and J. S. Colton, "On the structure of bulk and thin film Zn3As2 (in preparation)," (n.d.).
- D. D. Allred, R. S. Turley, S. M. Thomas, S. G. Willett, M. J. Greenburg, and S. B. Perry, "Adding EUV reflectance to aluminum-coated mirrors for space-based observation," Proc. SPIE 10398, 103980Y (2017).
- 17. J. Tauc, "Optical Properties of Amorphous Semiconductors and Solar Cells," in *Fundamentals of Semiconductors: Physics and Materials Properties*, P. Y. Cardona and M. Yu, eds. (Springer, 2012), pp. 566–568.
- J. Tauc, R. Grigorovici, and A. Vancu, "Optical Properties and Electronic Structure of Amorphous Germanium," Phys. Status Solidi B 15(2), 627–637 (1966).
- G. E. Jellison and F. A. Modine, "Parameterization of the optical functions of amorphous materials in the interband region," Appl. Phys. Lett. 69(3), 371–373 (1996).
- J. Orava, T. Wágner, J. Šik, J. Pĭikryl, M. Frumar, and L. Beneš, "Optical properties and phase change transition in Ge2 Sb2 Te5 flash evaporated thin films studied by temperature dependent spectroscopic ellipsometry," J. Appl. Phys. 104(4), 043523 (2008).
- G. D. Cody, "The Optical Absorption Edge of a-Si: H," in Semiconductors and Semimetals, Vol. 21, Hydrogenated Amorphous Silicon, Part B, Optical Properties (Academic Press, 1984), pp. 11–82.
- J. Price, P. Y. Hung, T. Rhoad, B. Foran, and A. C. Diebold, "Spectroscopic ellipsometry characterization of HfxSiyOz films using the Cody–Lorentz parameterized model," Appl. Phys. Lett. 85(10), 1701–1703 (2004).
- C. R. Henry, "Surface studies of supported model catalysts," Surf. Sci. Rep. 31(7-8), 231–325 (1998). See in particular Table 4 on page 258.
- D. G. Van Campen and J. Hrbek, "Silver on alumina: adsorption and desorption study of model catalysts," J. Phys. Chem. 99(44), 16389–16394 (1995).
- R. A. Rapp, J. P. Hirth, and G. M. Pound, "Condensation coefficients in the growth of cadmium and zinc from the vapor," J. Chem. Phys. 34(1), 184–188 (1961).
- M. Janai, D. D. Allred, D. C. Booth, and B. O. Seraphin, "Optical properties and structure of amorphous silicon films prepared by CVD," Sol. Energy Mater. 1(1-2), 11–27 (1979).
- W. A. McGahan, B. Johs, and J. A. Woollam, "Techniques for ellipsometric measurement of the thickness and optical constants of thin absorbing films," Thin Solid Films 234(1-2), 443–446 (1993).